THE ELECTROCHEMICAL PERFORMANCES OF Zr-BASED HYDROGEN STORAGE ALLOYS①

Yang, Xiaoguang Lei, Yongquan Wu, Jing Wang, Qidong
Department of Materials Science and Engineering, Zhejiang University, Hangzhou 310027

ABSTRACT The main crystal structure of $Zr(Cr_xNi_{1-x})_2$ ($X=0.15-0.65$) alloys prepared by the arc melting in an argon atmosphere was found to change from C15 to C14 as the ratio Cr/Ni increased, and the alloy $Zr(Cr_{0.35}Ni_{0.65})_2$ which was mainly of C15 exhibited maximum electrochemical discharge capacity of 305 mAh/g at 293 K. The exchange current density i_0 varied with the equlibrium potentials of the hydride electrodes, the lower the elctrode potentials, the larger the i_0 values. Fine alloy powders, especially those were pulverized in H_2 gas and the electrodes pretreated with (H_2O_2+HF) solution were highly activated. An obvioous variation of Zr $3d_{5/2}$ peak position before and after cyclings was detected, the discrepency is related with the activity of the hydride electrodes.

Key words Zr-based Laves phase crystal structure electrode performances

1 INTRODUCTION

Comparing with the convertional Cd-Ni rechargeable battery, the metal hydride-nickel (MH-Ni) secondary battery has higher energy density, high ability to stand overcharge and overdischarge, no heavy metal pollution and compatibility of battery potential. Until now many electrochemical studies have been carried out on the negative electrode materials such as AB_5, AB and AB_2 systems[1-3]. Zr-Ni (V) based AB_2 type Laves phase alloys had large hydrogen storage capacities, but their hydride electrodes exhibited low electrochemical discharge capacities due to the formation of the stable hydrides[4]. In order to reduce the stability of hydrides, later a study on the partial substitution of A and B in the same system was carried out and $Zr_{0.5}Ti_{0.5}(V_{0.375}Ni_{0.625})_2$ was found to have a higher capacity (349 mAh/g at a discharge current density of 16 mA/g)[5]. The hydrogen capacity of this alloy was satisfatory but its electrode stability was poor. It was the severe dissolution of V and Ti in KOH that deterioted the electrode life. It appears to us that it is worthy to carry out the study on the electrochemical performances of Zr-Cr-Ni system alloy electrodes since $ZrCr_2$ has a large hydrogen capacity and is resistant to KOH solution. The present paper is a summary of our investigation and some results of XPS analysis are also reported.

2 EXPERIMENTAL DETAILS

The alloys were prepared by arc melting under an Ar atmosphere using the pure constitutent metals Zr, Cr, Ni (purity > 99.0%). The alloys in as-cast state were crushed mechanically to make the alloy powders all pass through −360 mesh sieve. XRD were obtained from −360 mesh unactivated alloy powders using Rigaku C/max-Ⅲ B diffractormeter with a Cu Kα radiation and a nickel diffracted-beam filter.

The hydride electrodes were prepared by cold pressing the mixtures of different alloy powder (−360 mesh) with powdered electrolytic copper (1:2 in a weight ratio) to form porous pellets with d10 mm in copper holders. The discharge capacities were determined by galvanostatic method in an opened standard

① Supported by "863" program; Received Jul. 28, 1994; accept Nov. 12, 1994

trielectrode cell, the counter-electrode was nickel oxyhydroxide, reference electrode was Hg/HgO/6 mol/L KOH and the electrolyte was 6 mol/L KOH solution. The electrodes were fully charged at a current density of 100 mA/g for 4.5h and discharged at 50mA/g and cut-off potential set at −0.60V *vs.* Hg/HgO. The discharge curves were recorded by a LM15 type X-Y recorder. A HDV-7B potentiatist and a KEITHLEY multimeter with a $5^1/2$ accuracy were adopted in the experiment.

The alloy electrode samples were analyzed with XPS before and after electrochemical cycles. The measurements were performed using a VG ESCALB MK Ⅱ electron spectrometer. Al Kα radiation was used for XPS and the C1*s* peak(285.0eV) as the calibration of energy position. The sputter depth profiles (Ar^+, 4keV) were evaluated using at standard rate of 80 Å/min.

3 RESULTS AND DISCUSSION

Fig. 1 represents XRD patterns for $X=0.35$ and 0.6 of $Zr(Cr_XNi_{1-X})_2$ alloys. As the composition of Cr increases and Ni decreases, the lattice parameters of the tricomponent system alloys increases, see Table 1. This phenomenon is ascribed to the geometric effect of atomic radii. Transition from face centre cubic C15 to hexagonal C14 Laves phase occurs at about the composition range of $X=0.4-0.5$. In Fig. 1(a) the major phase is of typical C15 structure, the extra small peak around $2\theta=37.50°$ is identified to be that of the secondary phase compound $ZrNi_X$ ($X=1\sim2$). Fig. 1(b) shows C14 hexagonal structure without $ZrNi_X$ phase. The existence of the secondary phase was believed to be benificial to the activity of the hydride electrodes[6].

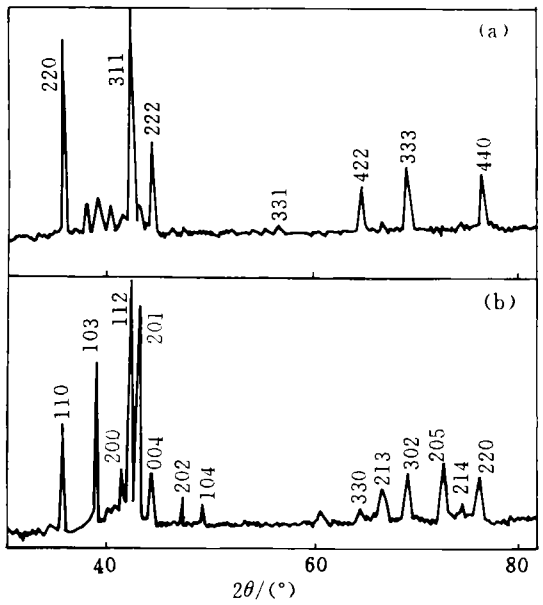

Fig. 1 XRD of $Zr(Cr_XNi_{1-X})_2$ alloys
(a)—C15, $X=0.35$; (b)—C14, $X=0.6$

Table 1 Crystal structures and lattice constants in $Zr(Cr_XNi_{1-X})_2$ syatem alloys

Alloy	main phase	a/Å	c/Å
$Zr(Cr_{0.2}Ni_{0.8})_2$	C15	7.008	
$Zr(Cr_{0.25}Ni_{0.75})_2$	C15	7.023	
$Zr(Cr_{0.33}Ni_{0.67})_2$	C15	7.051	
$Zr(Cr_{0.35}Ni_{0.65})_2$	C15	7.054	
$Zr(Cr_{0.4}Ni_{0.6})_2$	C15	7.057	
$Zr(Cr_{0.45}Ni_{0.55})_2$	C15	7.068	
$Zr(Cr_{0.5}Ni_{0.5})_2$	C14	5.009	8.329
$Zr(Cr_{0.6}Ni_{0.4})_2$	C14	5.016	8.347
$Zr(Cr_{0.6}Ni_{0.4})_2$	C14	5.025	8.344

Fig. 2 represents the dependence of hydrogen capacities on the composition. There is a sharp decrease in the region $X<0.33$, and

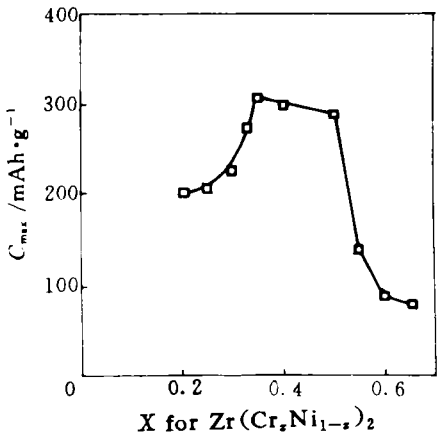

Fig. 2 Capacity charge C_{max} with composition for $Zr(Cr_XNi_{1-X})_2$ dischsrge at 50mAg, 298K

discharge capacity reaches a maximum of 305 mAh/g at $X = 0.35$ and 298K. The increase of Cr concentration leads a significant decrease in electrochemical discharge capacity, since the amount of electrocatalytic Ni decreases and the stabler hydrides are formed.

The reaction of hydride electrodes contains two steps: (1) the electron transfer in the interface of electrodes and electrolytes; (2) hydregon absorbed on the surface of the hydride particles diffuses inside. The electrode process will be controlled by the electrochemical reaction when the discharge current density is low enough, the overpotential η is low as well, that is $\eta \ll RT/\beta nF$ (about 50 mV). The exchange current density i_0 of the electrode can be obtained as following[7]:

$$i_0 = RT\, i/F\eta \quad (\mathrm{mA/g}) \qquad (1)$$

where i and η are the discharge current density and corresponding overpotential respectively; R, T, F are gas constant, absolute temperature and Falady constant

Fig. 3 depicts the relationship between overpotential and discharge current of the hydride electrodes with different equilibrium potentials . The exchange current density i_0 are obtained from the slopes of lines, which vary with the equilibrium potentials of the electrodes, see Table 2.

Table 2 The equilibrium potentials and excharge current density of electrodes with different hydrogen concentration

Hydride electrodes	Equilibrium potentials(V)	Excharge current density i_0 (A/g)
$ZrCr_{0.5}Ni_{1.5}$	−0.975 0	0.014 51
	−0.812 7	0.000 612 0
$ZrCr_{0.7}Ni_{1.3}$	−0.942 1	0.023 20
	−0.809 6	0.002 820

The activity of hydride electrodes is an important factor for electrode performances. Modifying the surface of the electrodes, i. e. oxidation treatment in O_2 atmosphere, change alloys composition especially surface components, was found to be easy to activate the electrodes. Fig. 4 shows the dependence of activity on particle size of alloy $Zr(Cr_{0.5}Ni_{0.5})_2$. The electrode with +140 mesh powder in the first cycles exhibits dischargeability comparable with that of −360 mesh powder, but its C_i/C_{max} (discharge capacity in the charge-discharge cycle to the maximum capacity) in-

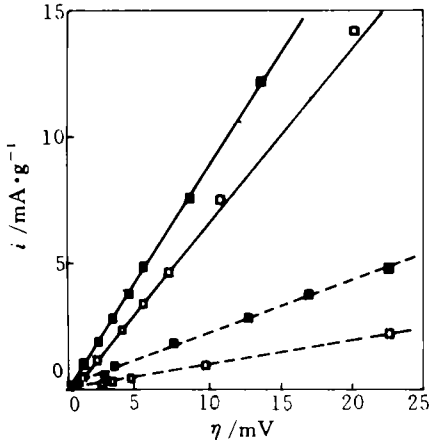

Fig. 3 The relationship between equilibrium potential and anodic current density(i) of the electrode $Zr(Cr_xNi_{1-x})_2$ *vs.* Hg/HgO η 298 K

□— $X = 0.25$, Ueq — −0.975 0 V ··· −0.812 7 V
□— $X = 0.35$, Ueq — −0.942 1 V ··· −0.809 6 V

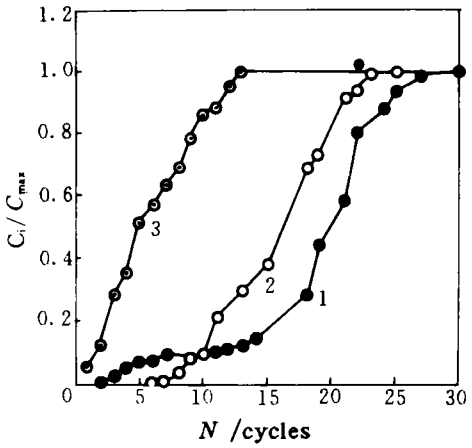

Fig. 4 Activity property dependence of alloy particle size of ZrCrNi

1—+140 mesh; 2——360 mesh;
3——360 mesh(pulverized by cycling in hydrogen gas)

creases slowly in the following 15 cycles. In comparision with the electrode formed from powder grinded mechanically, another electrode was formed with the same alloy powder pulverized by cycling in H_2 gas and shows favorite activity. The improvement is tentatively attributed to the formation of much more defects after cyclings, which reduce the barrier for charging hydrogen. It is interesting to see that the electrodes with the same particle size have similar slope increment $d(C_i/C_{max})/d N$.

Fig. 5 shows the cathodic polarization curves and discharge curves of $Zr(Cr_{0.35}Ni_{0.65})_2$ electrodes pretreated with $(HF+H_2O_2)$. Both electrodes were prepared by first pasting a colloidal mixture of alloy powders and PVA glue of 3% concentration onto a foamed Ni plate and then cold pressing. The untreated one shows a larger cathodic overpotential than the treated one in the same cathodic currents shown in Fig. 4. This indicates that the former has difficulty in absorbing hydrogen in KOH solution to form hydrides because of the generation of H_2 gas. It is worthy to note that the initial capacity of the treated one reaches 110 mAh/g while another shows no capacity at all. It can be concluded that the treatment improves activity, or that the surface state of alloy electrodes greatly affects the polarization performance and hydrogen electrochemical chargeability.

Fig. 6 illustrates XPS patterns for Zr, Cr and Ni core peaks before and after electrochemical cyclings. The XPS patterns for the uncycled ZrCrNi electrode consists of $Zr3d_{5/2}$ peak at 186.5 eV, $Cr3p_{3/2}$ at 576.5 eV and Ni $3P_{3/2}$ at 856.2 eV. It is worthy to note that the 186.5 eV of Zr $3d_{5/2}$ is not found to be suitable to any compounds in the XPS data manual, and the careful energy calibration against C1s (285.0 eV) is performed; However, the peak position of Zr $3d_{5/2}$ in the activated one shifts to 183.6 eV and Ni $3p_{3/2}$ shows no evident position change, but the $Cr3p_{3/2}$ peak is not able to detected. According to the analyses of the O1s, we can conclude that the metal oxides are spread over the surface of the uncycles alloy powders and the metal hydroxide exist in that of the cycled ones. There is an obvious shift of Zr 3d peak, which is due to the difference in structure of Zr oxide layer. After sputtering off 70 Å the Zr 3d peaks of both samples arrive at 183.0 eV. It appears that the layer within 50 Å or so plays an important role in activation process. This layer can be

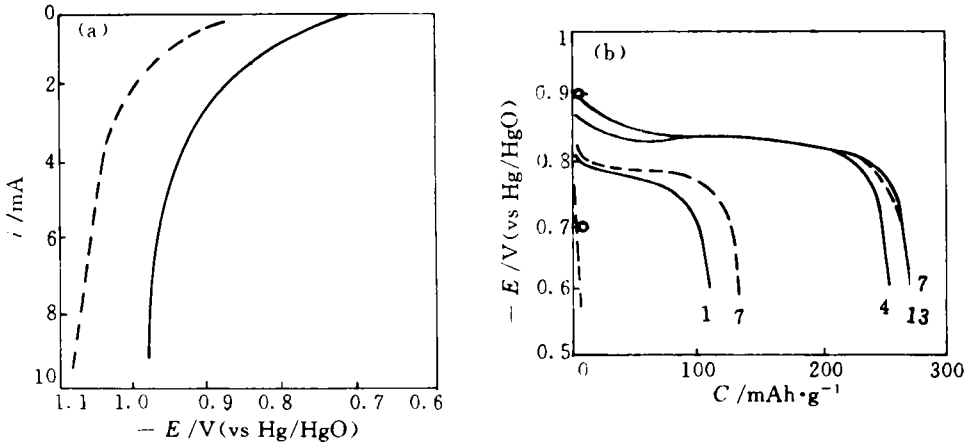

Fig. 5 Cathodic polarization curves 1 mV/s, 298 K (a) and Discharge curves at difference cycle number of $ZrCr_{0.7}Ni_{1.3}$ electrode, 50 mA/g, 298 K (b)

disbed line—untreated; solid line—surface treated with $(HF+H_2O_2)$ solution

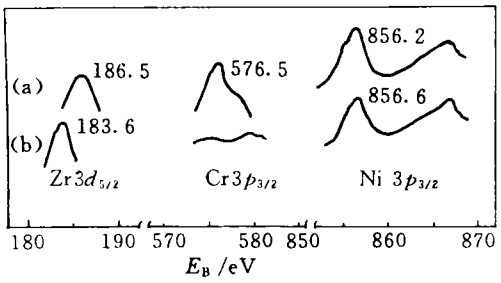

Fig. 6 XP spetra for virgin, activated eletrode surfaces

(a)—virgin; (b)—activated electrode surfaces

removed by the above treatment, thus the treatment also modifies the activity as mentioned above. But the activation mechanism need to be further studied.

4 CONCLUSION

(1) The main crystal structure of the Zr $(Cr_XNi_{1-X})_2$ ($X = 0.15 \sim 0.65$) changes from C15 to C14 at $X = 0.4 \sim 0.5$, and the alloy Zr $(Cr_{0.35}Ni_{0.65})_2$ has the maximum electrochemical discharge capacity of 305 mAh/g at ambient temperature.

(2) Activation process is accelerated by immersing the electrodes in $(HF + H_2O_2)$ solution as well as cycling in gaseous H_2. The effect of later is more obvious.

(3) The XPS analyses demonstrate a segregation of Zr on activated sample, the structres of surface oxides are believed to be important for activation.

REFERENCES

1 Willems J J. Philips J Res, 1984, 39(1): 1.
2 Reichman *et al.* US 4716 088, 1987.
3 Sakai T *et al.* Prog Batteries Sol Cell, 1990, 9: 269.
4 Sawa H *et al.* Materials Trans JIM, 1990, 31(6): 487.
5 Sawa H *et al.* Denki Kagaku, 1991, 59(11): 945.
6 Kim S R *et al.* J Alloys & Compounds, 1992, 185: L1—L4.
7 Tian Zhaowu. the Methods of the Electrochemical Study. Science Press,